Experimental investigation of the effects of using metal-oxides/water nanofluids on a photovoltaic thermal...

Article *in* Energy · July 2017

DOI: 10.1016/j.energy.2017.07.046

CITATIONS
0

READS
69

4 authors, including:

Mohammad Sardarabadi
Ferdowsi University Of Mashhad
11 PUBLICATIONS **111** CITATIONS
SEE PROFILE

Mohammad Hosseinzadeh
Ferdowsi University Of Mashhad
2 PUBLICATIONS **0** CITATIONS
SEE PROFILE

Arash Kazemian
Ferdowsi University Of Mashhad
1 PUBLICATION **0** CITATIONS
SEE PROFILE

Energy 138 (2017) 682–695

Contents lists available at ScienceDirect

Energy

journal homepage: www.elsevier.com/locate/energy

Experimental investigation of the effects of using metal-oxides/water nanofluids on a photovoltaic thermal system (PVT) from energy and exergy viewpoints

Mohammad Sardarabadi*, Mohammad Hosseinzadeh, Arash Kazemian, Mohammad Passandideh-Fard

Department of Mechanical Engineering, Ferdowsi University of Mashhad, Mashhad, Iran

ARTICLE INFO

Article history:
Received 21 January 2017
Received in revised form
10 June 2017
Accepted 9 July 2017
Available online 12 July 2017

Keywords:
Photovoltaic thermal system
Metal-oxides/water nanofluids
Energy and exergy analysis
Entropy generation

ABSTRACT

In this paper, an experimental investigation on the effects of using metal-oxides/water nanofluids as a coolant system in a photovoltaic thermal system (PVT) from the energy and exergy viewpoints are presented. The considered nanoparticles include Al_2O_3, TiO_2 and ZnO dispersed in deionized water as the base fluid by 0.2 wt%. A constant mass flow rate of 30 kg/h for the fluid flowing through the collector is considered. The experiments are performed on selected days in August and September at the Ferdowsi University of Mashhad, Mashhad, Iran. The uncertainty of the experiments is less than 5%. The measured data are analyzed from the energy/exergy viewpoints and entropy generation. Based on the extensive results presented in this paper, the PVT/ZnO and PVT/TiO_2 systems show a better overall energy and exergy efficiencies compared to other systems. The results indicate that the overall exergy efficiencies for the cases of PVT/water, PVT/TiO_2, PVT/Al_2O_3, and PVT/ZnO are enhanced by 12.34%, 15.93%, 18.27% and 15.45%, respectively, compared to that of the photovoltaic unit (PV) with no collector. Moreover, the PVT/Al_2O_3 system has the highest enhancement of entropy generation compared to the PV unit.

1. Introduction

Due to the limitations of the fossil fuels resources and their adverse effects on the environment such as global warming, ozone layer depletion, and climate changes [1,2]; there is a growing intention to find new methods to extract sustainable renewable energy sources. The biggest source of the renewable energies, available freely throughout the year, is the sun. A photovoltaic thermal system (PVT) consists of a common photovoltaic unit (PV) which transforms photons received by the sun into electrical energy, and a thermal collector which absorbs both remaining energy of photons and the heat generated by photovoltaic cells. Simultaneous generation of electricity and useful thermal energy makes these types of solar systems more efficient compared to a conventional PV unit with no collector. Increasing the surface temperature of the PV unit reduces the electrical efficiency of the PV unit by nearly 0.45% for each degree rise in temperature [3,4]. Consequently, cooling the PV unit is an effective method for improving the power output without damaging the PV unit [5].

Many factors can affect thermal and electrical efficiencies of PVT systems. These factors are classified into two main categories, external and internal. External factors such as solar irradiation intensity and ambient temperature depend on climate conditions, while internal factors such as thermal collector structure and cooling fluid type depend upon the system design. In order to evaluate the effect of external and internal factors on improving the performance of PVT systems, energy and exergy analyses are required. The performance of the system cannot be evaluated by an energy analysis alone because it does not consider the direction of process, the quality of energies, and internal irreversibilities [6]. Therefore, an exergy analysis is also necessary to investigate the real performance of PVT systems [6]. It should be noted that the exergy of PVT systems can be determined from two viewpoints, net output exergy and exergy losses [6,7]. Numerous studies available in the literature attempted to improve the efficiency of PVT systems by changing the internal and external factors. Fujisawa and Tani [8] evaluated the exergy efficiency of a PVT water system, experimentally. They concluded that the PVT water system has more output exergy compared to that of a PV unit or a flat plate solar collector. Chow et al. [9] studied the effect of glass cover on energy

* Corresponding author.
E-mail address: m.sardarabadi@yahoo.com (M. Sardarabadi).

http://dx.doi.org/10.1016/j.energy.2017.07.046
0360-5442/

Nomenclature

A	Area (m^2)
Be	Bejan number
C_f	Conversion factor
C_P	Specific heat capacity (J kg^{-1} K^{-1})
$\dot{E}$	Power (W)
$\dot{E}''$	Power per unit area (W m^{-2})
$\dot{E}x$	Exergy rate (W)
$\dot{E}x''$	Exergy rate per unit area (W m^{-2})
$\dot{E}^*_{el}$	The electrical power with regard to the pump consumption (W)
FF	Fill factor
$\dot{G}$	Incident radiation rate (W)
$\dot{G}''$	Incident radiation rate per unit area (W m^{-2})
h	Enthalpy (J kg^{-1})
I	Electrical current (A)
$\dot{m}$	Mass flow rate (kg s^{-1})
P	Pressure (Pa)
PV	Photovoltaic unit
PVT	Photovoltaic thermal system
R	Arbitrary function
$R\dot{E}_{out,\max}$	A certain amount of required power (W)
r	Packing factor
s	Entropy (J kg^{-1} K^{-1})
T	Temperature (K)
V	Electrical voltage (V)
$\dot{E}_{out,1m^2}$	Output electrical power from a unit area of the PV unit (W)

Greeks

α	Absorptivity
η	Energy efficiency (%)
η^*_{el}	The electrical efficiency with regard to the pump consumption
ε	Exergy efficiency (%)
δ	Uncertainty
ρ	Density (kg m^{-3})
ϕ	Nanoparticles volume fraction in the base fluid
υ	Arbitrary parameter
τ	Glass cover transmissivity
ψ	stream exergy per unit mass

Subscripts

amb	Ambient
bf	Base fluid
c	Collector
$cell$	Photovoltaic cell
eff	Effective
el	Electrical
f	Fluid
fr	Friction
g	Glass cover
gen	Generate
in	Input
$m\ ax$	Maximum
n	Nanoparticle
oc	Open circuit
out	Outlet
ov	Overall
p	Pump
pv	Photovoltaic unit
pvt	Photovoltaic thermal system
Q	Heat transfer
i	Counter
sc	Short circuit
t	Time
th	Thermal
tot	Total

and exergy of a thermosiphon-based water heating PVT system. They found that the energy efficiency of the glazed system is more than that of the system with no glass cover. For the exergy efficiency, however, the unglazed system (with no glass cover) is found to be more efficient. Mishra and Tiwari [10] presented energy and exergy analyses for a water PVT system at a constant collection temperature mode (a constant outlet temperature). They considered two different cases, a collector partially covered by a PV unit and a collector fully covered. They concluded that the annual overall exergy output is increased by 39.16% for the collector fully covered by a PV unit. Wu et al. [11] presented several procedures for evaluating heat and exergy losses of conventional PVT systems in a review article. Yazdanpanahi et al. [6] investigated the exergy efficiency of a water PVT system both numerically and experimentally. They reported an optimum value of the mass flow rate for which the exergy efficiency is maximum. Hazami et al. [12] analyzed the performance of a PVT system under Tunisian climatic conditions for both passive and active modes. They found maximum instantaneous thermal and electrical energy efficiencies in active mode to be about 50 and 15%, respectively. They also reported maximum thermal and electrical exergy efficiencies of 50 and 14.8%, respectively.

Generally, fluids have a lower thermal conductivity compared to solid metals [13]. Therefore, dispersion of metal-oxide nanoparticles in a fluid increases its thermal conductivity and heat transfer performance. In addition, the convective heat transfer coefficient of nanofluids is higher than that of conventional fluids. Hence, one technique to improve the performance of PVT systems is using nanofluids. The main problem of using nanofluids in these systems is the limited time of their stability [14]. Moreover, the pressure drop in nanofluids is increased due to nanoparticles. This drawback, however, is usually ignored compared to their heat transfer enhancement [15]. Several attempts have been made to study the effect of nanofluids on the performance of solar systems. Mahendran et al. [16] experimentally studied the performance of an evacuated tube solar collector using water-based nanofluids. They reported a maximum total efficiency of 73% for the PVT system using a 0.3 wt% TiO_2/water nanofluid. They also found that using Al_2O_3/water nanofluid can increase the efficiency by 8% compared to TiO_2/water nanofluid. Said et al. [17] studied a flat plate solar collector using TiO_2/water nanofluid. The highest energy efficiency they reported was 76.6% for the nanofluid with 0.1% volume fraction and 0.5 kg/min flow rate. They also achieved a maximum exergy efficiency of 16.9% for the same conditions. Al-Shamani et al. [18] performed experimental studies on a rectangular tube absorber photovoltaic thermal collector with various types of nanofluids under tropical climate conditions. They reported a thermal and electrical efficiency of 63.67% and 10.53%, respectively, for a TiO2/water nanofluid with a flow rate of 0.068 kg/s. Elmir et al. [19] numerically studied the performance of a PVT system using

Al_2O_3/water nanofluid. They concluded that the heat transfer is significantly improved in comparison with pure water. They also investigated the effect of nanoparticles volume fraction for different values of Reynolds number on the performance of the system. Xu and Kleinstreuer [20] presented a numerical and experimental study of nanofluid effect on a concentrating PVT system (referred as CPVT) performance for different climatic conditions. They compared the annual electrical output of the PV unit with various working fluids, and found that the annual performance of the CPVT nanofluid is higher than that of the conventional system. Sardarabadi et al. [14] performed a numerical and experimental study of various metal oxides/water nanofluids with 0.2 wt %. They observed that TiO_2/water and ZnO/water nanofluids have a better electrical efficiency compared to Al_2O_3/water nanofluid. They also found the highest thermal efficiency for the ZnO/water nanofluid. Khanjari et al. [21] analyzed the performance of a PVT system using Al_2O_3/water nanofluid, numerically. They evaluated the effects of two operating parameters including the solar irradiation and coolant inlet temperature. Using the Al_2O_3/water nanofluid improved the heat transfer coefficient and efficiency of the system compared to water.

Based on the second law of thermodynamics, the minimization of entropy generation in a system translates into the minimum exergy losses of the system due to irreversibilities. Few studies on entropy generation for PVT systems are available in the literature; nevertheless, there exist many investigations that analyzed entropy generation in other systems such as solar collectors. Leong et al. [22] performed an entropy generation analysis of a nanofluid flow in a circular duct subjected to a constant wall temperature. Their study focused on Al_2O_3/water and TiO_2/water nanofluids. They observed that the total dimensionless entropy generation is reduced with an increase of nanoparticle volume fractions. Also, they found that a higher length and diameter of the collector tube, and a lower mass flow rate of the nanofluid results in a less entropy generation. Bianco et al. [23] proposed an entropy generation of a turbulent convection flow of Al_2O_3/water nanofluid in a circular tube subjected to a constant outer heat flux. Their analysis was performed for a constant mass flow rate ranged from 0.3 to 0.5 kg/s and a nanoparticle concentration ranged from 0% to 6%. Based on their results, a simple way to reduce the entropy generation for a constant Reynolds number is adding nanoparticles to the working fluid. Mahian et al. [24] presented a detailed review of the entropy generation in various nanofluids applications. Alim et al. [25] analytically investigated the entropy generation and pressure drop in a conventional flat plate solar collector using Al_2O_3/water, CuO/water, SiO_2/water, TiO_2/water nanofluids with a volume fraction of 1–4% for nanoparticles. The entropy generation was decreased with increasing the nanoparticle volume fractions. Based on their results, the CuO/water nanofluid could decrease the entropy generation by 4.34% in comparison with pure water. Said et al. [26] studied the effect of single wall carbon nanotubes (known as SWCNTs) based nanofluids on the performance of a flat plate solar collector. They observed that for the same base fluid, the SWCNTs have the minimum entropy generation compared to Al_2O_3, TiO_2 and SiO_2 nanoparticles. Vijayalakshmi et al. [27] presented an experimental study of entropy generation in a PVT water system. They found the entropy generation to be minimum for a mass flow rate of 0.008 kg/s.

In this paper, the effects of using three metal-oxides/water nanofluids by 0.2 wt% on both thermal and electrical efficiencies are experimentally investigated. The considered nanoparticles include: Aluminum-oxide (Al_2O_3), Titanium-oxide (TiO_2) and Zinc-oxide (ZnO). The experiments are performed at a constant mass flow rate. To investigate the reliability of the measurements, an uncertainty analysis is performed for the experimental data which shows an uncertainty of less than 5% for all the cases considered. The main focus of this study is to investigate the actual performance of a PVT system with a flat plate collector from the exergy viewpoint. As mentioned earlier, few studies on entropy generation for PVT systems are available in the literature. Thus, the effects of using three metal-oxides/water nanofluids on the exergy losses and entropy generation of the PVT system are evaluated.

2. Experimental setup and nanofluid preparation

In this study, the experimental setup consists of two 40W mono-crystalline silicon photovoltaic modules (Suntech Co., China). One module is equipped with a sheet-and-tube collector, while the other has no collector. The PV unit is attached to the top surface of a thin copper plate soldered on the back to a serpentine copper tubing with a thermal insulation layer beneath. The design of the absorber collector is shown in Fig. 1-a. Properties and design parameters of the PVT system are provided in Table 1. The two considered systems are tested under identical conditions. They are tilted toward the south with a constant tilt angle of 30°. The schematic diagram and a view of the experimental setup are shown in Fig. 1b–c. The working fluid is stored in a tank (2.5 Lit capacity) connected to a pump (AC - 220 V - 13 W) in order to circulate the fluid around the panel with a steady constant mass flow rate of 30 kg/h. To have a closed flow circuit for the working fluid, a shell-and-tube heat exchanger with a counter flow design is used to cool the working fluid after being heated in the PVT collector. Additionally, the second fluid used in the heat exchanger is the running city water with a 40 kg/h mass flow rate. It has been shown elsewhere [28] that these flow rates result in the highest system efficiency. A rotary flow meter (LZB10-20 to 60 Lit/h) is used to measure and fix the flow rate at a constant value. Pressure at the inlet and outlet of the collector are measured by a pressure transmitter (Atek-100 mbar). Moreover, flow temperatures at the inlet and outlet of the collector, and PV surface temperature are measured and saved by K-types sensors with a data logger (Testo-177-T4, UK). Two digital multimeters (UT 71C/D/E) are used to measure short-circuit currents and open-circuit voltages. The total incident radiation is measured by a solar power meter (TES-1333, Taiwan) mounted parallel to the photovoltaic surfaces. The working fluids considered in the experiments are pure water, Al_2O_3/water, TiO_2/water and ZnO/water nanofluids. Transmission electron microscope (TEM) images of the Al_2O_3, TiO_2 and ZnO nanoparticles are shown in Fig. 2, a-c, indicating that the nanofluids consist of spherical particles with a diameter size and properties reported in Table 2. All nanoparticles are dispersed in deionized water with 0.2 wt% by a high-speed stirrer and a proper surfactant. Surfactants for the Al_2O_3, TiO_2 and ZnO, were: Nitric acid [29], Acetic acid [30,31], and Ammonium citrate [32,33], respectively. The mixture is then stabilized under a continuous sonication using an ultrasound vibrator (Wisd DH.WUC.D10H, Korea) at a set constant temperature of 60 °C. The ultrasonic process time is divided into six-time periods of 20 min. To examine the nanofluids stability, the density of the nanofluid at various locations and times during the course of the experiment is measured. For the duration of each experiment (6 h), no significant changes in the density and sedimentation were observed. To have more reliable results and a less uncertainty, the daily measured data was collected from 9:30 a.m. to 3:30 p.m. on selected days in August and September at the Ferdowsi University of Mashhad, Mashhad, Iran (Latitude: 36° and Longitude: 59°).Sudden changes in weather conditions during a day, especially the solar irradiation due to clouds and ambient temperature can affect the result of the PVT system. Hence, the experiments for all working fluids are performed on several days with a similar

(a)

(b)

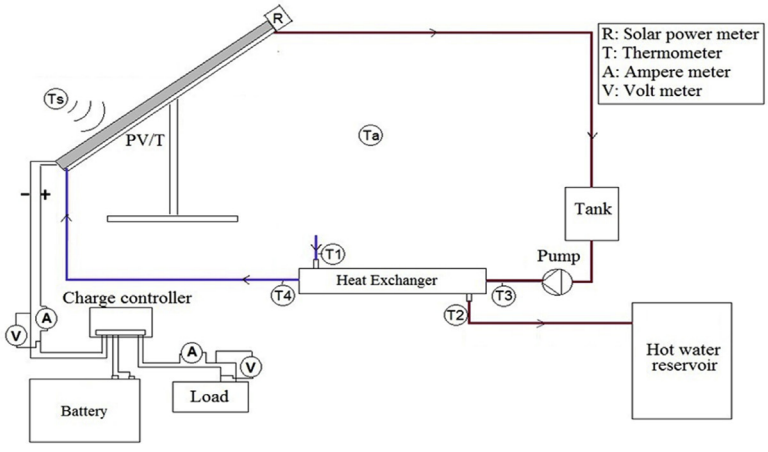

(c)

Fig. 1. (a) A view of the collector design, (b) A view and (c) schematic diagram of the experimental setup.

weather conditions. Subsequently, the measured data are averaged before being applied in the calculations. The performance of a PVT system depends on solar irradiation. Based on the location (Mashhad, Iran) and the weather conditions, the optimum solar irradiation for the thermal collector operation is selected from 9:30 a.m. to 3:30 p.m. (six hours for each day). It should be noted that although a PVT system can be used in other times during the day, the pumping power required to circulate the working fluid

Table 1
Properties and design parameters of PVT system.

Photovoltaic solar cell (Under standard test conditions)	
Type	Mono-crystalline silicon
Maximum power (W)	40
Cell dimension (mm)	62.5×125
Number of cells	36
Fill factor	0.726
Open circuit voltage (V)	21.6
Short-circuit current (A)	2.57
Optimum power voltage (V)	17.6
Optimum operating current (A)	2.29
Cell efficiency (QUOTE %)	16
Module efficiency (QUOTE %) QUOTE	15
Tempered glass thickness (mm)	3
Flat plate collector	
Type	Sheet-and-tube
Tube material	Copper
effective area of each collector (m^2)	0.3
Sheet thickness (mm)	0.4
Inner diameter of pipes (mm)	10
External diameter of pipes (mm)	12
Insulation Thickness (mm)	30
Packing factor	1

will not be compensated by the output of the PVT system; i.e., the net power output of the system will be negligible.

3. Thermodynamic analysis

The second law analysis is required to determine the performance of the PVT systems because it is more realistic and it considers the quality of energies as well [6].

3.1. Energy analysis

The energy flow diagram of a PVT system is schematically displayed in Fig. 3. Based on this figure, considering the PV unit and the thermal collector as a united control volume and assuming a steady state condition, the energy balance for this control volume, can be expressed as [28]:

$$\begin{aligned} &\sum \dot{E}_{in} = \sum \dot{E}_{out} + \sum \dot{E}_{loss} \\ &\Rightarrow \dot{E}_{sun} + \dot{E}_{mass,in} = \dot{E}_{el} + \dot{E}_{mass,out} + \dot{E}_{loss} \end{aligned} \quad (1)$$

where, $\dot{E}_{in}$, $\dot{E}_{out}$ and $\dot{E}_{loss}$ refer to energy rate related to the input, output and losses, respectively. In this equation, $\dot{E}_{sun}$ is equal to the effective incident solar radiation, $\dot{G}_{eff}$, to the PVT system that can be expressed as:

$$\dot{E}_{sun} = \dot{G}_{eff} = \tau_g \cdot \alpha_{cell} \cdot \dot{G} \quad (2)$$

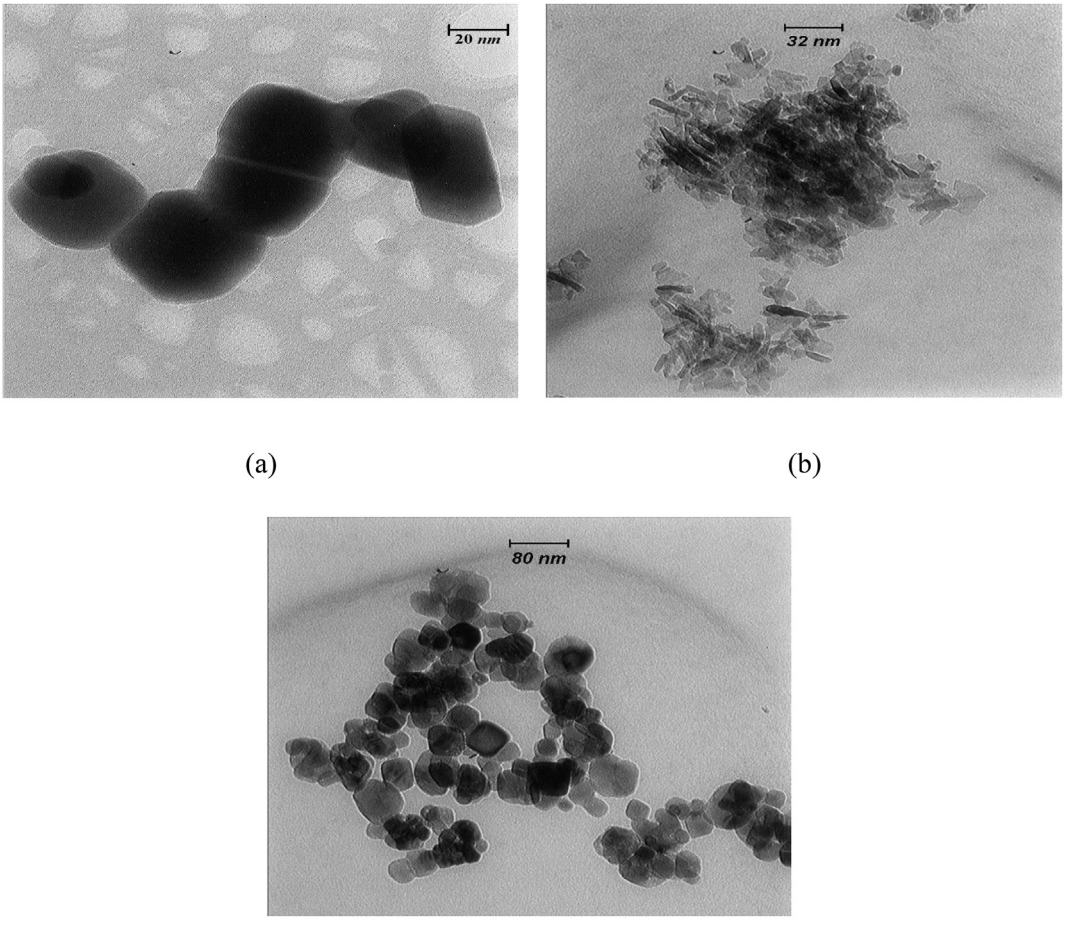

Fig. 2. TEM of the (a) ZnO, (b) Al_2O_3 and (c) TiO_2 nanoparticles (central laboratory of Ferdowsi University of Mashhad).

Table 2
Nanoparticles proprieties.

Nanoparticle	Particle size (nm)	Density (kg m^{-3})	Heat capacity (J kg^{-1} K^{-1})	Thermal conductivity (W m^{-1} K^{-1})
Al_2O_3	10–30	3970	765	40
TiO_2	20–60	4250	686	8.9
ZnO	35–45	5600	495	13

where, τ_g is the glass cover transmissivity, α_{cell} the cell absorptivity and $\dot{G}$ is the rate of the total incident radiation. In Eq. (1), energy in connection with the mass flow rate can be calculated as follows:

$$\dot{E}_{mass,out} - \dot{E}_{mass,in} = \dot{m}_f \cdot C_{p,f} \cdot \left(T_{f,out} - T_{f,in}\right) \tag{3}$$

where, $\dot{m}_f$, $C_{p,f}$, $T_{f,in}$ and $T_{f,out}$ are the mass flow rate through the collector, specific heat capacity and the inlet and outlet temperatures of the working fluid, respectively. It is obvious that Eq. (3) indicates the useful thermal energy rate of the system absorbed by the working fluid. If a nanofluid is used as the working fluid, thermo-physical properties of the prepared nanofluid can be calculated using the base fluid and nanoparticles characteristics at the bulk temperature, using following equations [34]:

$$C_{p,nf} = \frac{\phi \cdot (\rho_n \cdot C_{p,n}) + (1-\phi) \cdot \left(\rho_{bf} C_{p,bf}\right)}{\rho_{nf}} \tag{4}$$

$$\rho_{nf} = \phi \cdot \rho_n + (1-\phi) \cdot \rho_{bf} \tag{5}$$

where, ρ is the density and subscripts n, bf and nf represent nanoparticles, base fluid and nanofluid, respectively. ϕ , is the volumetric ratio of nanoparticles in the base fluid that can be calculated by following expression [35]:

$$\phi = \frac{m_n/\rho_n}{m_n/\rho_n + m_f/\rho_f} \tag{6}$$

where, m_n and m_f are the mass of the nanoparticles and the base fluid, respectively. $\dot{E}_{el}$, is the output electrical power of the PV unit which can be calculated based on following equation:

$$\dot{E}_{el} = V_{oc} \times I_{sc} \times FF \tag{7}$$

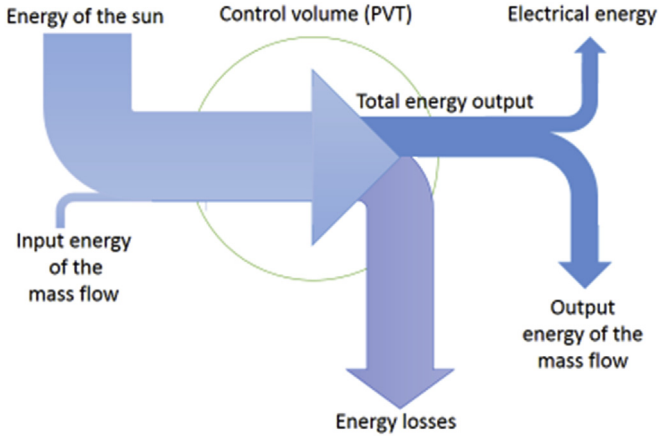

Fig. 3. Energy flow diagram of a PVT system.

where, V_{oc} and I_{sc} are the open circuit voltage and short circuit current of the PV unit, respectively. *FF* (fill factor) is defined as the maximum power conversion efficiency of the PV unit that can be evaluated based on the ratio of the maximum power gained from the photovoltaic module to the open circuit voltage multiplied by the short circuit current at the standard test condition of the PV unit [36]:

$$FF = \frac{\dot{E}_{el,\max}}{V_{oc} \times I_{sc}} = \frac{V_{\max} \times I_{\max}}{V_{oc} \times I_{sc}} \tag{8}$$

In this equation, V_{oc} and I_{sc} are the open circuit voltage and short circuit current that have constant values. They are given at the standard test condition by the manufacturer. The overall efficiency of a PVT system, η_{ov}, is equal to the ratio of the output power to the sun power during a selected time period. Thus, the overall efficiency can be written as a function of thermal and electrical efficiencies (η_{th} and η_{el}) [9]:

$$\eta_{ov} \cong \frac{\dot{E}_{th} + \dot{E}_{el}}{\dot{E}_{sun}} \Rightarrow \eta_{pvt} = \frac{\int_{t1}^{t2} \left(A_c \dot{E}''_{th} + A_{pv} \dot{E}''_{el}\right) dt}{A_c \int_{t1}^{t2} \left(\dot{G}''_{eff}\right) dt} = \eta_{th} + r \cdot \eta_{el} \tag{9}$$

where, A_c and A_{pv} are the collector and PV unit areas, respectively and r is the packing factor defined as PV unit area to the collector area (A_{pv}/A_c). $\dot{E}''_{th}$ is the rate of the output thermal power per unit area of the collector, $\dot{E}''_{el}$ the rate of the output electrical power per unit area of the PV unit and $\dot{G}''_{eff}$ is the rate of incident radiation per unit area of the collector.

In Eq. (9), the electrical and thermal efficiencies can be expressed as:

$$\eta_{el} = \frac{\dot{E}_{el}}{\dot{E}_{sun}} = \frac{V_{oc} \times I_{sc} \times FF}{\dot{G}_{eff}} \tag{10}$$

$$\eta_{th} = \frac{\dot{E}_{th}}{\dot{E}_{sun}} = \frac{\dot{m}_f \cdot C_{p,f} \cdot \left(T_{f,out} - T_{f,in}\right)}{\dot{G}_{eff}} \tag{11}$$

In order to analyze the PVT system based on the thermal power, the output electrical power must be converted into thermal power for which a conversion factor C_f has been used in the literature [37,38]. The electrical and overall equivalent PVT powers can be calculated as:

$$\dot{E}_{el,th} = \frac{\dot{E}_{el}}{C_f} \tag{12}$$

$$\dot{E}_{ov,th} = \dot{E}_{th} + \dot{E}_{el,th} \tag{13}$$

In the most PVT systems, a value of C_f has been considered between 0.35 and 0.40 [38]. Therefore, in the present study, it is considered to be 0.38 [28]. Thus, the electrical and overall equivalent PVT efficiencies can be modified as the following:

$$\eta_{el,th} = \frac{\eta_{el}}{C_f} \tag{14}$$

$$\eta_{ov,th} = \eta_{th} + r \cdot \eta_{el,th} \tag{15}$$

Considering the electrical power required for fluid pumping, we have:

$$\dot{E}_{el}^{*} = \dot{E}_{el} - \dot{E}_{p} \tag{16}$$

where $\dot{E}_{el}$ is the output electrical power of the PVT system determined using Eq. (7) and $\dot{E}_{p}$ is the electrical power required for pumping calculated as [6]:

$$\dot{E}_{p} = \frac{\dot{m}\Delta P}{\rho_{nf}\eta_{p}} \tag{17}$$

where ΔP and η_{p} are pressure drop in the PVT collector and pump efficiency, respectively. The electrical efficiency of the PVT system, therefore, is obtained as follows [6]:

$$\eta_{el}^{*} = \frac{\dot{E}_{el} - \dot{E}_{P}}{\dot{G}_{eff}} \tag{18}$$

3.2. Exergy analysis and entropy generation

The exergy analysis is performed similar to the energy analysis. Fig. 4 shows the exergy flow diagram of a PVT system. Considering the PV unit and the thermal collector as a single control volume and assuming a steady state condition, the exergy balance can be expressed as follows:

$$\begin{aligned} &\sum \dot{E}x_{\,in} = \sum \dot{E}x_{\,out} + \sum \dot{E}x_{\,loss} \\ &\Rightarrow \dot{E}x_{\,sun} + \dot{E}x_{\,mass,in} = \dot{E}x_{\,el} + \dot{E}x_{\,mass,out} + \dot{E}x_{\,loss} \end{aligned} \tag{19}$$

where, $\dot{E}x_{\,in}$, $\dot{E}x_{\,out}$ and $\dot{E}x_{\,loss}$ refer to exergy rate of input, output and losses, respectively. Incident solar radiation to the system is used to calculate the rate of the sun exergy, $\dot{E}x_{\,sun}$ [2]:

$$\dot{E}x_{sun} = \dot{G}\left(1 - \frac{T_{amb}}{T_{sun}}\right) \tag{20}$$

where, T_{amb} and T_{sun} are the temperature of the ambient and the sun (as a black body $T_{sun} \cong 5800K$), respectively. The exergy of the mass flow rate can be defined as [2,26]:

$$\dot{E}x_{\,mass,out} - \dot{E}x_{\,mass,in} = \dot{m}_{f}(\psi_{out} - \psi_{in}) \tag{21}$$

where:

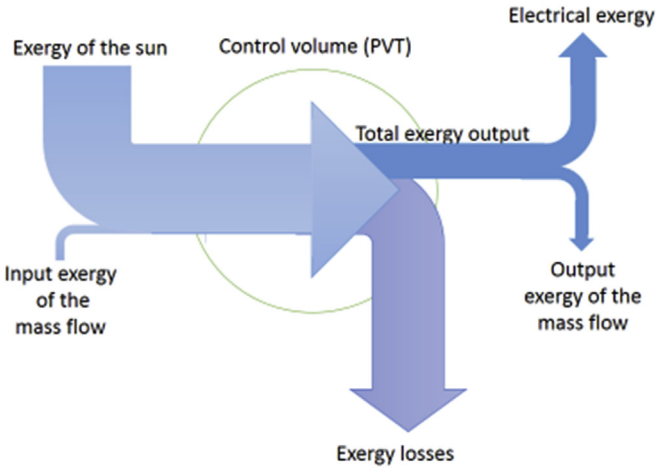

Fig. 4. Exergy flow diagram of a PVT system.

$$\psi_{out} = (h_{out} - h_{amb}) - T_{amb}(s_{out} - s_{amb}) \tag{22}$$

$$\psi_{in} = (h_{in} - h_{amb}) - T_{amb}(s_{in} - s_{amb}) \tag{23}$$

where, h and s are the enthalpy and entropy values. Because the electrical energy is a useful available work, the exergy of the PV unit is equal to the electrical power [9]:

$$\dot{E}x_{\,el} = \dot{E}_{el} \tag{24}$$

By substituting Eqs. (20)–(23) into Eq. (19), we have:

$$\left(1 - \frac{T_{amb}}{T_{sun}}\right)\dot{G} - \dot{E}_{el} - \dot{m}_{f}[(h_{out} - h_{in}) - T_{amb}(s_{out} - s_{in})] = \dot{E}x_{\,loss} \tag{25}$$

In this equation, the entropy and enthalpy changes of the fluid flow can be defined as [2]:

$$\Delta h = h_{out} - h_{in} = C_{p,f}\left(T_{f,out} - T_{f,in}\right) \tag{26}$$

$$\Delta s = s_{out} - s_{in} = C_{p,f} ln\left(\frac{T_{f,out}}{T_{f,in}}\right) \tag{27}$$

It should be noted that $\dot{E}_{loss}$ and $\dot{E}x_{\,loss}$ in Eq. (1) and Eq. (19) are only due to heat transfer losses. Therefore, these two terms in the rest of the formulations will be indicated with $\dot{E}_{loss,Q}$ and $\dot{E}x_{\,loss,Q}$, respectively. There is another exergy loss in the PVT system due to fluid friction in the collector which can be defined as the following [39]:

$$\dot{E}x_{\,loss,fr} = \frac{\dot{m}_{f}\Delta P}{\rho_{f}} \frac{T_{amb} \cdot ln\left(\frac{T_{f,out}}{T_{f,in}}\right)}{\left(T_{f,out} - T_{f,in}\right)} \tag{28}$$

where, ΔP is the pressure drop in the collector. The rate of total entropy generation of the selected control volume can be obtained as [26]:

$$\begin{aligned} \dot{S}_{gen,tot} &= \frac{\dot{E}x_{\,loss,tot}}{T_{amb}} = \frac{\dot{E}x_{\,loss,Q} + \dot{E}x_{\,loss,fr}}{T_{amb}} = \frac{\dot{E}x_{\,loss,Q}}{T_{amb}} + \frac{\dot{E}x_{\,loss,fr}}{T_{amb}} \\ &= \dot{S}_{gen,Q} + \dot{S}_{gen,fr} \end{aligned} \tag{29}$$

where, $\dot{S}_{gen,tot}$, $\dot{S}_{gen,Q}$ and $\dot{S}_{gen,fr}$ refer to the rate of total entropy generation, entropy generation due to heat transfer, and entropy generation due to fluid friction, respectively. In order to compare the contribution of heat transfer and fluid friction in the total entropy generation, the Bejan number is expressed as the following [39]:

$$Be = \frac{\dot{S}_{gen,Q}}{\dot{S}_{gen,tot}} \tag{30}$$

Similar to Eq. (9), the overall exergy efficiency of the PVT system can be written as a function of thermal and electrical exergy efficiencies [9]:

$$\varepsilon_{ov} \cong \frac{\dot{E}x_{th} + \dot{E}x_{el}}{\dot{E}x_{sun}} \Rightarrow \varepsilon_{ov} = \frac{\int_{t1}^{t2}\left(A_c \dot{Ex}''_{th} + A_{pv}\dot{Ex}''_{el}\right)dt}{A_c\int_{t1}^{t2}\left(\dot{Ex}''_{sun}\right)dt} = \varepsilon_{th} + r\varepsilon_{el} \quad (31)$$

where, $\dot{Ex}''_{th}$ is the rate of the output thermal exergy per unit area of the collector, $\dot{Ex}''_{el}$ is the rate of the output electrical exergy per unit area of the PV unit and $\dot{Ex}''_{sun}$ is the rate of the sun exergy per unit area of the collector.

In Eq. (31), the electrical and thermal exergy efficiencies can be expressed as:

$$\varepsilon_{el} = \frac{\dot{E}x_{el}}{\dot{E}x_{sun}} = \frac{\dot{E}_{el}}{\dot{G}\left(1 - \frac{T_{amb}}{T_{sun}}\right)} = \frac{V_{oc} \times I_{sc} \times FF}{\dot{G}\left(1 - \frac{T_{amb}}{T_{sun}}\right)} \quad (32)$$

$$\varepsilon_{th} = \frac{\dot{E}x_{th}}{\dot{E}x_{sun}} = \frac{\dot{m}_f \cdot C_{p,f}\left[\left(T_{f,out} - T_{f,in}\right) - T_{amb} ln\left(\frac{T_{f,out}}{T_{f,in}}\right)\right]}{\dot{G}\left(1 - \frac{T_{amb}}{T_{sun}}\right)} \quad (33)$$

4. Uncertainty analysis

In order to determine the reliability of the experiments, an uncertainly analysis is performed for the measured parameters and electrical efficiency [28]. The uncertainties associated with the measuring instruments of the experimental setup are reported in Table 3. If R is a function of 'n' independent linear parameters as $R = R(v_1, v_2, ..., v_n)$, the uncertainty of function R is defined as:

$$\delta R = \sqrt{\left(\frac{\partial R}{\partial v_1}\delta v_1\right)^2 + \left(\frac{\partial R}{\partial v_2}\delta v_2\right)^2 + ... + \left(\frac{\partial R}{\partial v_n}\delta v_n\right)^2} \quad (34)$$

where δR is the uncertainty of function R, δv_i the uncertainty of parameter v_i, and $\frac{\partial R}{\partial v_i}$ is the partial derivative of R with respect to parameter v_i. The uncertainty of the experiments was found to be less than 5% for all cases in this paper. More details regarding the uncertainty analysis can be seen elsewhere [28].

5. Results and discussion

The average daily summaries of the measured weather data during the experiments are presented in Fig. 5. According to this figure, the average ambient temperature and incident irradiation are 33.42 °C and 917 W/m^2, respectively. The maximum incident irradiation occurs at 1:00 p.m. which is equal to 1059 W/m^2.

5.1. Energy analysis

As mentioned before, in order to improve the performance of a PV unit, i.e., to increase its electrical output, the system can be equipped with a collector (PVT) through which a working fluid circulates to cool down the photovoltaic cells. The average cell temperature difference between the PVT system and PV unit for various nanofluids is represented in Fig. 6. It should be noted that in this figure, delta T is the temperature difference between the surface temperature of the PVT system and that of the PV unit. This figure shows that adding nanoparticles to pure water decreases the surface temperature. In addition, the results reveal that in all cases, the PVT/ZnO system has the lowest surface temperature compared to other cases. The higher enhancement of the coolant thermal conductivity and the convective heat transfer for nanofluids compared to those of the base fluid has been correlated to several

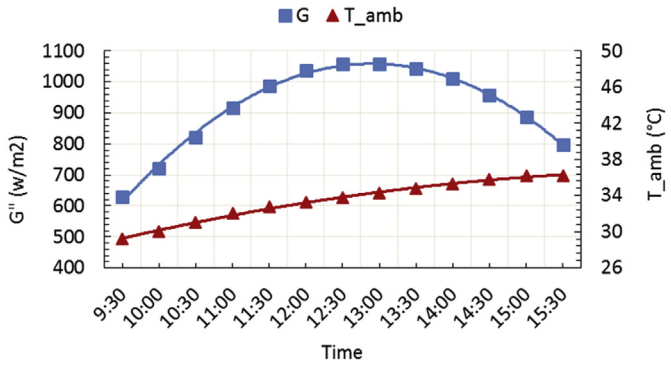

Fig. 5. Average daily variation of the total incident radiation and ambient temperature during the test period.

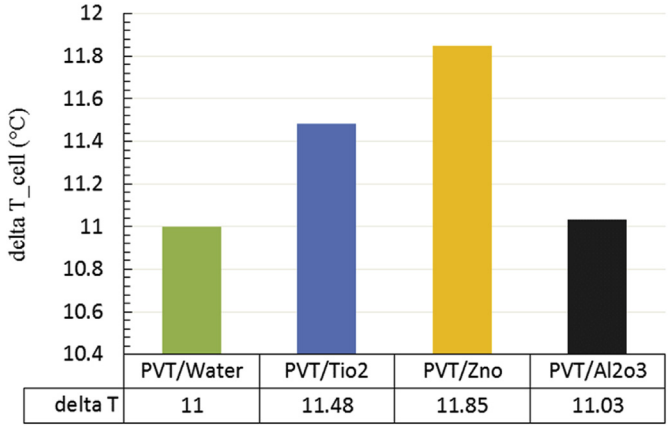

Fig. 6. Average temperature difference between PVT systems and PV unit for various nanofluids.

Table 3
Measuring equipments and their uncertainties.

Equipment and model	Measurement section	Accuracy	Maximum uncertainty (in experiments)
Digital multimeter (UT 71C/D/E)	Voltage (Open circuit and load)	±(0.5% + 1)	0.06 V
Digital multimeter (UT 71C/D/E)	Ampere (short circuit and load)	±(0.8% + 1)	0.02 A
Pyranometer (TES-1333)	Incident solar radiation	±10 W/m^2 +0.38 W/m^2 (*for* T_{ref} + 1 °C)	5.8 W/m^2
K-types thermocouple	Fluid and PV surface temperature	±0.25 °C	0.14 °C
Hg thermometer	Ambient temperature	±0.5 °C	0.3 °C
Rotameter (LZB10)	Mass flow rate	±2 kg/h	1.15 kg/h
Pressure transmitter (Atek - 100 mbar)	Fluid pressure	±0.5% *for* 25 °C	0.22 mbar

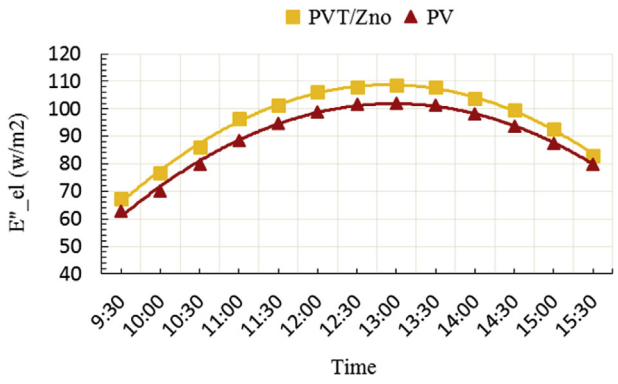

Fig. 7. Electrical power of PV unit and ZnO nanofluid during the daily experiment.

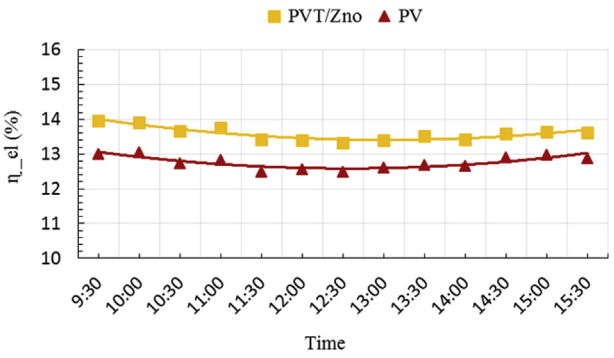

Fig. 9. Electrical energy efficiency of the system during the daily experiment.

mechanisms such as nanoparticle migration, nanoparticle clustering, and Brownian motion of nano particles [40–43]. In a numerical study performed by Sardarabadi et al. [14], they also observed the lowest surface temperature for the PVT/ZnO system compared to other cases they considered.

Fig. 7 displays the electrical power calculated using Eq. (7) for both the PVT/ZnO system and PV unit during the daily experiments. As demonstrated in the figure, using a nanofluid enhances the electrical power since the surface temperature is lowered compared to that of the PV unit. This is due to the enhancement of the coolant thermal conductivity and the convective heat transfer between the coolant and the collector. Furthermore, the average electrical power using the ZnO/water nanofluid is 95.19 W/m^2 indicating that the electrical power is increased by nearly 6.73% compared to that of the PV unit. It is also observed in the figure that due to a maximum irradiation, the electrical power is maximized at 1:00 p.m.

Fig. 8 illustrates the variation of the thermal and electrical powers by using Eq. (3) and Eq. (7), respectively, during the daily experiment (9:00 a.m. to 3:30 p.m.) for different cases (i.e., PVT/water, PVT/ZnO, PVT/Al_2O_3, PVT/TiO_2 and PV systems). According to the figure, using nanofluids in the PVT system enhances the thermal power by 31.01%, 34.31%, and 8.12% for the cases of PVT/TiO_2, PVT/ZnO, and PVT/Al_2O_3 systems, respectively, compared to that of the PVT/water system. Particle migration, nanoparticle clustering, viscosity gradient and Brownian motion are several mechanism identified in the literature as the probable reasons for the thermal power enhancement of the PVT system [40–43]. This figure also shows that the electrical power compared to that of the PV unit system is increased by 5.33%, 6.99%, 6.73%, and 5.50% for the cases of PVT/water, PVT/TiO_2, PVT/ZnO, and PVT/Al_2O_3, respectively.

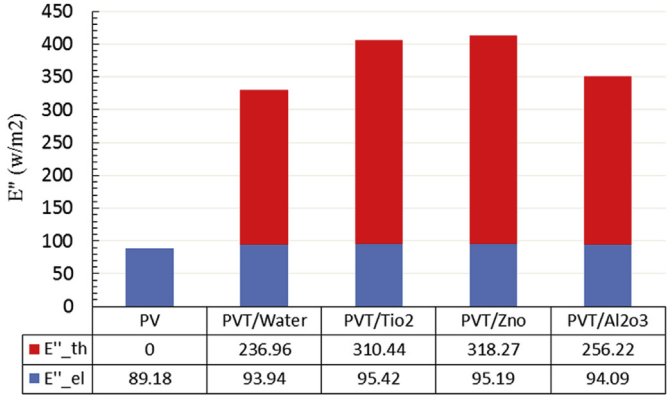

	PV	PVT/Water	PVT/Tio2	PVT/Zno	PVT/Al2o3
E"_th	0	236.96	310.44	318.27	256.22
E"_el	89.18	93.94	95.42	95.19	94.09

Fig. 8. Average thermal and electrical power during the daily experiment.

According to these results, the highest electrical power enhancement is observed for PVT/TiO_2 system, and the PVT/ZnO system exhibits the highest thermal power enhancement. Although a more reduction is observed for the average cells surface temperature for the ZnO/water nanofluid, the average electrical power of the TiO_2/Water is higher. This is due to a more uniform distribution in the cells surface temperature reduction for the TiO_2/water nanofluid compared to that of the ZnO/water.

The variation of the electrical efficiency using Eq. (10) is shown in Fig. 9 for the case with the ZnO/water nanofluid. As seen from the figure, using the nanofluid enhances the electrical efficiency since the surface temperature is lowered compared to that of the PV unit. The average electrical efficiency for the case of the PVT/ZnO is 13.59%, whereas, this amount for the PV unit is almost 12.73%. This means that by using the ZnO/water nanofluid, about 6.75% improvement in the electrical efficiency is observed. Moreover, by getting closer to the solar noon, the increasing rate of the electrical energy is much lower than that of the solar radiation due to a high temperature of the solar cells and their low performance. Therefore, the minimum electrical efficiency of the system is obtained at the solar noon.

In Fig. 10, the average electrical and thermal efficiencies using Eq. (10) and Eq. (11)are displayed during the daily experiments for different cases. As shown in the figure, the daily thermal and electrical efficiencies for pure water are found to be 34.12% and 13.41%, respectively. These values can be compared with the measurements performed by Chow et al. [9] where the average instantaneous thermal and electrical energy efficiencies during the daily experiment were reported to be 41% and 13.6%, respectively. In the experiment performed by Chow et al. [9], the working fluid

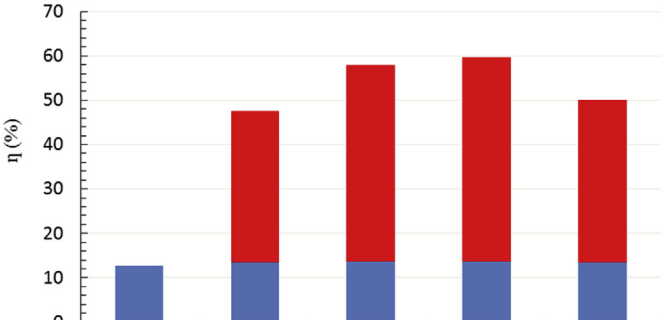

	PV	PVT/Water	PVT/Tio2	PVT/Zno	PVT/Al2o3
η_th	0	34.12	44.34	46.05	36.66
η_el	12.73	13.41	13.63	13.59	13.44

Fig. 10. Average of electrical and thermal energy efficiency of the system for different cases.

was pure water and the cooling system, similar to the present study, was a sheet-and-tube collector attached to the PV unit. Moreover, the results of the present study are in good agreement with those of Gang et al. [44] who reported a range of 25–75% and 4–13% for the thermal and electrical efficiencies of a water based PVT system, respectively. The amount of relative increase of thermal efficiency compared to that of the PVT/water for the cases of the PVT/TiO_2, PVT/ZnO, and PVT/Al_2O_3 are 29.95%, 34.96 and 7.44%, respectively. In addition, the average daily electrical efficiencies for the same three systems is increased by 7.06%, 6.75%, and 5.57%, respectively. Using a nanofluid as the working fluid results in a further decrease of the surface temperature compared to that of the PVT/water and PV unit (see Fig. 6); thus, the electrical efficiency is found to be higher when a nanofluid is used. Fig. 10 also indicates that the PVT/TiO_2 and PVT/ZnO systems have a better performance compared to other systems with an overall energy efficiencies (sum of electrical and thermal energy efficiencies) of 57.97% and 59.64%, respectively.

For a better comparison between various cases explained, the average electrical equivalent power and energy efficiency based on Eq. (13) and Eq. (15) during the daily experiments are summarized in Table 4. As shown in the table, cooling the PV unit increases both the electrical equivalent power and the electrical equivalent energy efficiency of these systems. The electrical equivalent power is increased by 5.34%, 6.99%, 6.73%, and 5.50% for the cases of PVT/water, PVT/TiO_2, PVT/ZnO, and PVT/Al_2O_3, respectively, in comparison with that of the PV unit. Moreover, the electrical equivalent energy efficiency compared to that of the PV unit is increased by 5.40%, 7.07%, 6.77%, and 5.61% for the cases of PVT/water, PVT/TiO_2, PVT/ZnO, and PVT/Al_2O_3, respectively. Consequently, the electrical equivalent power and energy efficiency for the PVT/TiO_2 system is higher.

Table 5 shows the effect of required power for fluid pumping through the collector on electrical power and electrical efficiency of the PVT system. As observed, the effect of pumping power on output electrical power and electrical efficiency for all cases is less than 1%. As a result, the energy required for fluid pumping through the PVT system has been neglected in the present study.

5.2. Exergy analysis

As it was mentioned earlier, the second law of thermodynamics determines the actual performance of the systems. Hence, in this section, by using the second law of thermodynamics, the exergy analysis results are presented. According to Eq. (20), the daily variation of the sun exergy during the experimental period is shown in Fig. 11. According to this figure, the minimum, maximum and average sun exergies are calculated to be 595, 1002 and 868 W/m^2, respectively.

In order to evaluate the quality of the electrical and thermal energies, the electrical and thermal exergies of the PVT system with four working fluids (pure water and TiO_2/water, ZnO/water, Al_2O_3/water nanofluids) are presented in Fig. 12a–d. It should be noted that in this case, the thermal exergy is calculated using Eq. (21). As shown in the figure, the thermal exergy of the PVT system is much lower than its electrical exergy. Consequently, the electrical energy has a higher quality compared to the thermal energy. In addition, the maximum electrical and thermal exergies are achieved at the solar noon due to increasing the solar irradiation. It is concluded that cooling the PV unit by using nanofluids is an efficient mechanism to improve the electrical exergy of the system. The average increase in the electrical exergy of the PVT system compared to that of the PV unit is 5.34%, 7%, 6.74% and 5.51% for pure water, TiO_2/water, ZnO/water and Al_2O_3/water, respectively. Although a more reduction is observed for the average cells surface temperature for the ZnO/water nanofluid, the average electrical exergy of the TiO_2/Water is higher. This is due to a more uniform distribution in the cells surface temperature reduction for the TiO_2/water nanofluid compared to that of the ZnO/water.

The average daily thermal exergy of the PVT systems with pure water, TiO_2/water, ZnO/water and Al_2O_3/water are compared in Fig. 13. This figure shows that adding metal-oxides nanoparticles to pure water increases the thermal exergy of the PVT system. This is due to the enhancement of the coolant thermal conductivity and the convective heat transfer between the coolant and the collector. Furthermore, the figure reveals that among all cases of nanofluids, the ZnO/water nanofluid has the best thermal performance. On the other hand, the TiO_2/water is the worst from the exergy viewpoint.

In order to evaluate the daily electrical exergy efficiency variation of the PVT system, the corresponding value for the PVT/ZnO system, as an example, is presented in Fig. 14. According to the figure, adding a flat plate collector to the PV unit improves its electrical exergy efficiency. By getting closer to the solar noon, the increasing rate of the electrical exergy is much lower than that of the solar radiation due to a high temperature of the solar cells and their low performance. Therefore, the minimum electrical efficiency of the system is obtained at the solar noon. It should be noted that the minimum exergy efficiency of the PV unit and PVT/

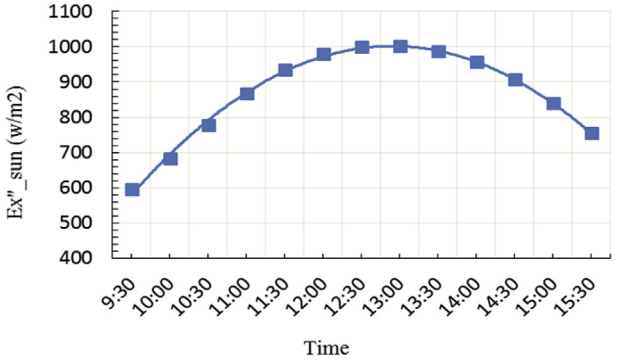

Fig. 11. The daily variation of the sun exergy.

Table 5
Investigation of the effect of required power for pumping on electrical power and electrical efficiency of the PVT system.

System type	PVT/Water	PVT/TiO_2	PVT/ZnO	PVT/Al_2O_3
$\dot{E}_{el}$	31.959	32.460	32.382	32.008
$\dot{E}^*_{el}$	31.948	32.449	32.372	31.998
η_{el} (%)	13.412	13.625	13.588	13.439
η^*_{el} (%)	13.408	13.620	13.584	13.434

Table 4
Average daily of overall equivalent power and overall equivalent energy efficiency of the systems.

System type	PV	PVT/Water	PVT/TiO_2	PVT/ZnO	PVT/Al_2O_3
Average electrical equivalent power (w/m^2)	234.68	247.22	251.09	250.49	247.6
Average electrical equivalent energy efficiency (%)	33.49	35.3	35.86	35.76	35.37

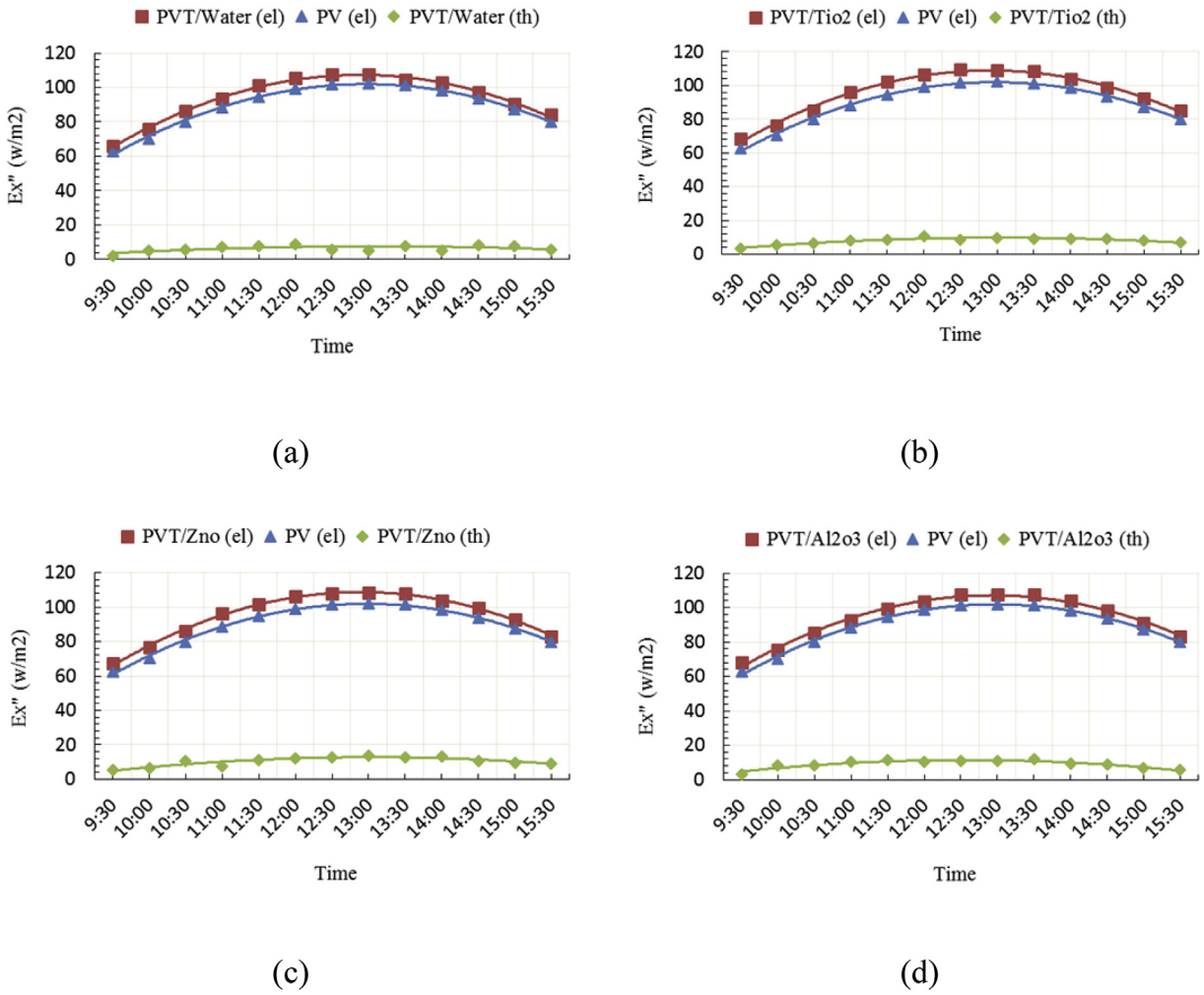

Fig. 12. The daily electrical and thermal exergies variation of the (a) PV and PVT/Water, (b) PV and PVT/TiO_2, (c) PV and PVT/ZnO and (d) PV and PVT/Al_2O_3 systems.

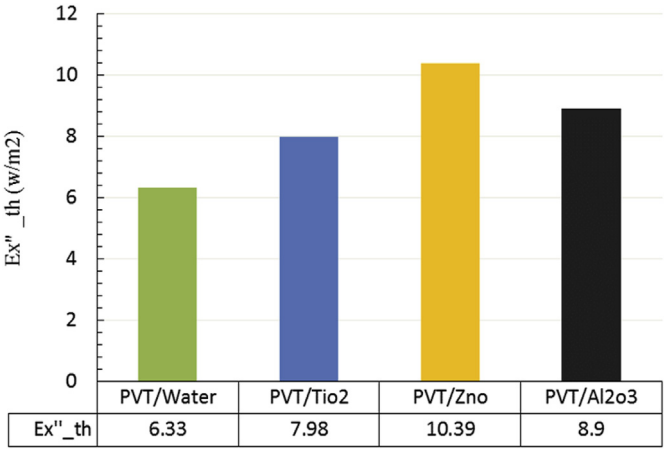

Fig. 13. Average daily thermal exergy of the PVT system.

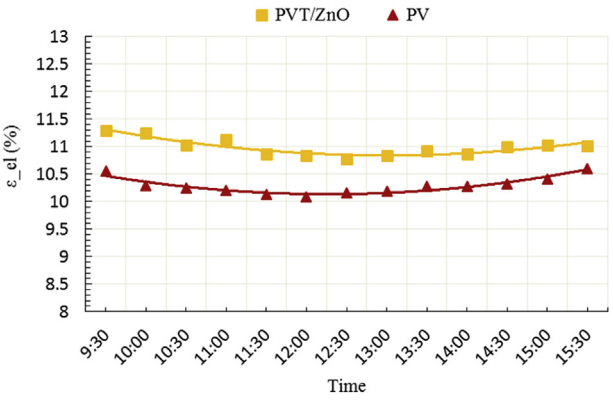

Fig. 14. Daily electrical exergy efficiency variation of the PVT/ZnO system.

ZnO system are about 10.09% and 10.77%, respectively.

In this study, the effect of working fluid on electrical and thermal exergy efficiencies of the PVT system is investigated in Fig. 15. This figure presents that the thermal exergy efficiency of the PVT system is extremely low due to low quality of the thermal energy. Using nanofluids in the PVT system enhances the performance of the system compared to the base fluid (pure water). This is due to the enhancement of the coolant thermal conductivity and the convective heat transfer between the coolant and the collector. The relative increase of the thermal exergy efficiency of nanofluids compared to that of pure water is 0.19%, 0.46% and 0.29% for TiO_2/water, ZnO/water and Al_2O_3/water, respectively. As seen in the figure, the overall exergy efficiencies for the cases of PVT/water, PVT/TiO_2, PVT/Al_2O_3, and PVT/ZnO are enhanced by 12.34%, 15.93%,

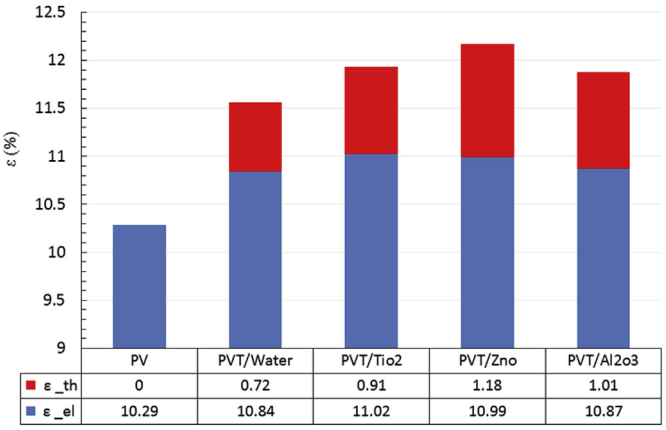

	PV	PVT/Water	PVT/Tio2	PVT/Zno	PVT/Al2o3
ε _th	0	0.72	0.91	1.18	1.01
ε _el	10.29	10.84	11.02	10.99	10.87

Fig. 15. Average daily thermal and electrical exergy efficiencies of the PV unit and PVT system.

18.27% and 15.45%, respectively, compared to those of the PV unit with no collector.

Calculating the entropy generation in each thermodynamic system can determine the amount of system losses and irreversibilities. Therefore, assessing the exergy loss and entropy generation in the PVT system is important. In the present study, as an example, a daily exergy loss of the PVT system due to heat transfer for the case of ZnO/water nanofluid using Eq. (25) is presented in Fig. 16. Based on the figure, the exergy loss in the PV unit and PVT system is high due to low overall exergy efficiency of the systems. Since the thermal exergy efficiency of the PVT system is extremely low, the exergy loss of the PV unit and PVT system are relatively close.

As it was mentioned earlier, the total entropy generation of the PVT system is due to heat transfer and fluid friction in the collector. A daily entropy generation variation due to heat transfer for the case of ZnO/water nanofluid is evaluated in Fig. 17. As shown in the figure, by getting closer to solar noon and increasing the cells surface temperature, the heat transfer between system and ambient and, therefore, the entropy generation is increased. It should be noted that an aggregation of nanoparticles in nanofluids can increase the irreversibility of the PVT system in a long time.

In order to have a better comparison of the PVT systems for four working fluids with each other and with that of the PV unit, the average daily of the sun energy and exergy, available energy and exergy, energy and exergy losses, entropy generation and the Bejan number during the experimental period are summarized in Table 6. The pressure drop for all working fluids is observed to be

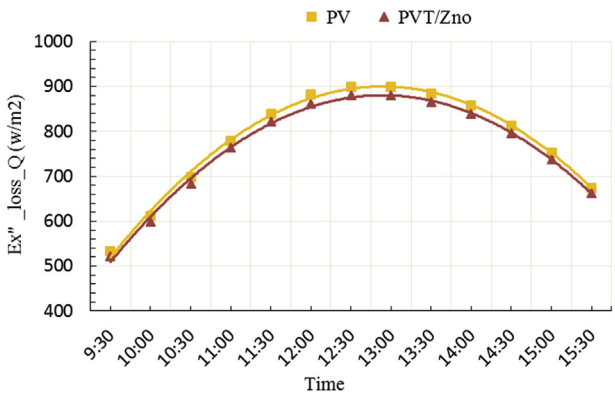

Fig. 16. Daily exergy loss variation of the PVT/ZnO system.

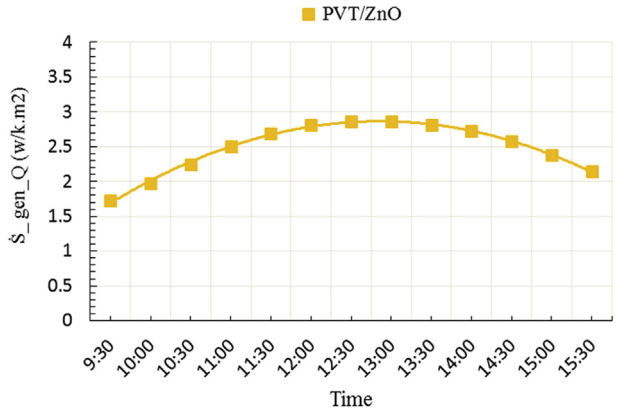

Fig. 17. Daily entropy generation variation of the PVT/ZnO system due to heat transfer.

approximately the same (around 1070 Pa). As the experimental conditions for all systems are the same; therefore, the average daily sun energy and exergy for all systems are 702 and 868 W/m^2, respectively. According to Table 6, a significant portion of the sun exergy in the PV unit is lost. By cooling the system in the PVT system, the exergy loss is reduced. Moreover, nanofluids are effective for more reduction of the exergy loss due to their enhancing effects on the heat transfer. Based on Eq. (28), since the mass flow rate and the difference between the inlet and outlet collector temperature is low, the exergy loss due to the fluid friction in the PVT system is small. It should be noted that the average daily exergy loss of the PVT system due to the fluid friction for all working fluids is about 0.025 W/m^2. Therefore, the entropy generation of the PVT systems due to the working fluid friction is negligible compared to that of the heat transfer. It can be concluded that the Bejan number in the PVT systems is approximately 1.In the case of nanofluids, the lowest exergy loss and entropy generation is achieved for the PVT/ZnO system. On the other hand, the Al_2O_3/water nanofluid has the highest value of exergy loss and entropy generation. This is due to the fact that PVT/Al_2O_3 system has lower both electrical and thermal exergy compared to other cases. Thus, according to Eqs. (25), (28) and (29), PVT/Al_2O_3 system has highest value of exergy loss and entropy generation. The reduction of the entropy generation in the PVT system compared to that of the PV unit is 1.42%, 1.85%, 2.09% and 1.77% for pure water and TiO_2/water, ZnO/water, Al_2O_3/water nanofluids, respectively.

5.3. Cost analysis

In order to have a general view of the cost saving, an energy and exergy analysis are performed based on the area reduction of each system in comparison with the PV unit (system without cooling). The size reduction of a system is an important factor for the economic analysis. Size reduction indicates how much the material can be saved with the same energy or exergy output of the system at the same condition. PV unit area (A_p) for producing a certain amount of required power ($R\dot{E}_{out,\max}$) can easily be calculated by Ref. [45]:

$$A_p = \frac{R\dot{E}_{out,\max}}{\dot{E}_{out,1m^2}} \tag{35}$$

where $\dot{E}_{out,1m^2}$ is output electrical power by a unit area of the PV module. In order to generate 1 kW electrical power, 46 PV units are required if each PV unit produces 40 W. From the energy viewpoint, by using pure water, PVT/TiO_2, PVT/ZnO and PVT/Al_2O_3, the size reduction of the PVT system compared to that of the PV is 21, 32, 33

Table 6
Average daily of the sun energy and exergy, available energy and exergy, energy and exergy loss, entropy generation and Bejan number of the systems.

System type	PV	PVT/Water	PVT/TiO_2	PVT/ZnO	PVT/Al_2O_3
Sun energy (W/m^2)	702	702	702	702	702
Sun exergy (W/m^2)	868	868	868	868	868
Available energy (W/m^2)	89.177	330.903	405.858	413.460	350.312
Available exergy (W/m^2)	89.177	100.274	103.394	105.580	102.990
energy loss_Q	612.823	371.097	296.142	288.54	351.688
Exergy loss_fr (W/m^2)	–	0.025	0.025	0.025	0.025
Exergy loss_Q (W/m^2)	778.823	767.726	764.606	762.420	765.010
Total exergy loss (W/m^2)	778.823	767.751	764.631	762.445	765.035
Ṡ_ gen_fr (W/k m^2)	–	8.343×10^{-5}	8.343×10^{-5}	8.282×10^{-5}	8.269×10^{-5}
Ṡ_ gen_Q (W/k m^2)	2.539	2.503	2.492	2.486	2.494
Be	–	≅ 1	≅ 1	≅ 1	≅ 1

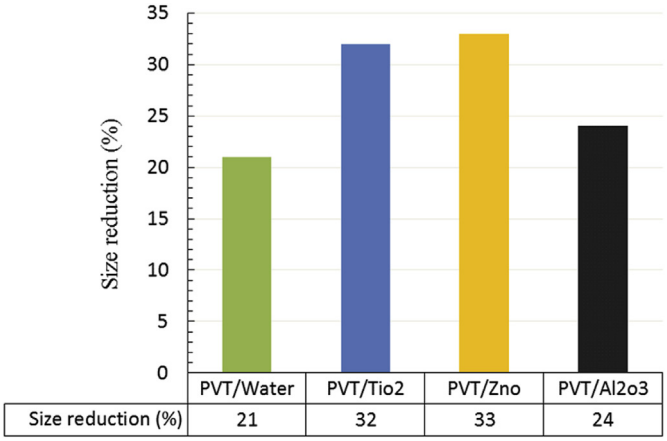

(a)

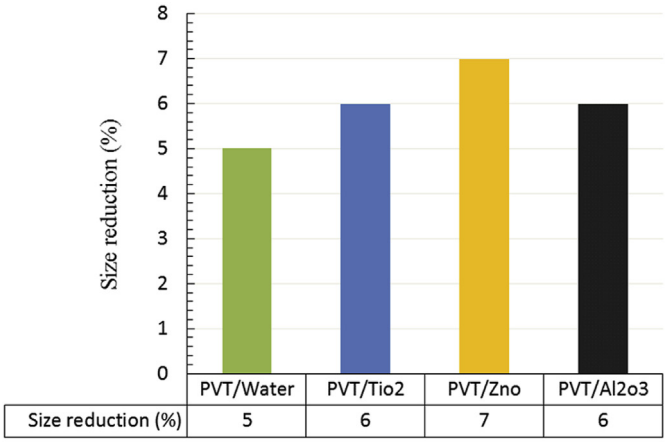

(b)

Fig. 18. Size reduction of PV module when using a PVT system from (a) energy and (b) exergy viewpoints.

and 24%, respectively (see Fig. 18-a). From the exergy viewpoint, the size reduction values are about 5, 6, 7, 6%, respectively (see Fig. 18-b). The small size reduction based on the exergy approach may be attributed to the small thermal exergy values.

6. Conclusions

In this study, the effects of using metal-oxides/water nanofluids as coolant on the performance of a PVT system, from the exergy viewpoint were experimentally investigated. The experiments were performed for four working fluids (pure water and TiO_2/water, ZnO/water, Al_2O_3/water nanofluids by 0.2 wt% concentration) on selected days in August and September at the Ferdowsi University of Mashhad, Mashhad, Iran. The investigated parameters in this study were cells surface temperature, electrical and thermal energy efficiencies, electrical and thermal exergy efficiencies, exergy loss and entropy generation. The experimental results of various nanofluids were compared with each other and with those of a PV unit. Based on the results, the following conclusions were made:

- Using nanofluids was effective in reducing the exergy loss and the entropy generation due to their heat transfer enhancement in PVT systems.
- ZnO/water and TiO_2/Water nanofluids were found to have an overall energy and exergy efficiencies higher than that of other cases.
- The exergy loss and entropy generation due to fluid friction in the PVT system was small. It should be noted that the average daily exergy loss of the PVT system due to fluid friction for all working fluids was 0.025 W/m^2. It was concluded that the Bejan number in the PVT system is approximately 1.
- As a result, regardless of the economic aspects of nanofluids preparation and nanofluid stabilization difficulties, using metal-oxides/water nanofluids enhance the performance of a PVT system both energetically and exergetically. Moreover it reduces the entropy generation of the system. The lowest exergy loss and entropy generation among various nanofluids considered in this paper was found to be for the PVT system with ZnO/water nanofluid.

References

[1] Höök M, Tang X. Depletion of fossil fuels and anthropogenic climate change—a review. Energy Policy 2013;52:797–809.
[2] Park SR, Pandey AK, Tyagi VV, Tyagi SK. Energy and exergy analysis of typical renewable energy systems. Renew Sustain Energy Rev 2014;30:105–23.
[3] Bai A, Popp J, Balogh P, Gabnai Z, Pályi B, Farkas I, et al. Technical and economic effects of cooling of monocrystalline photovoltaic modules under Hungarian conditions. Renew Sustain Energy Rev 2016;60:1086–99.
[4] Katkar A, Shinde N, Patil P. Performance & evaluation of industrial solar cell wrt temperature and humidity. Int J Res Mech Eng Technol 2011;1(1):69–73.
[5] Ma T, Yang H, Zhang Y, Lu L, Wang X. Using phase change materials in photovoltaic systems for thermal regulation and electrical efficiency improvement: a review and outlook. Renew Sustain Energy Rev 2015;43:1273–84.
[6] Yazdanpanahi J, Sarhaddi F, Mahdavi Adeli M. Experimental investigation of exergy efficiency of a solar photovoltaic thermal (PVT) water collector based on exergy losses. Sol Energy 2015;118:197–208.
[7] Sobhnamayan F, Sarhaddi F, Alavi MA, Farahat S, Yazdanpanahi J. Optimization of a solar photovoltaic thermal (PV/T) water collector based on exergy concept. Renew Energy 2014;68:356–65.
[8] Fujisawa T, Tani T. Annual exergy evaluation on photovoltaic-thermal hybrid

collector. Sol Energy Mater Sol Cells 1997;47(1):135–48.
[9] Chow TT, Pei G, Fong KF, Lin Z, Chan ALS, Ji J. Energy and exergy analysis of photovoltaic–thermal collector with and without glass cover. Appl Energy 2009;86(3):310–6.
[10] Mishra RK, Tiwari GN. Energy and exergy analysis of hybrid photovoltaic thermal water collector for constant collection temperature mode. Sol Energy 2013;90:58–67.
[11] Wu S-Y, Guo F-H, Xiao L. A review on the methodology for calculating heat and exergy losses of a conventional solar PV/T system. Int J Green Energy 2015;12(4):379–97.
[12] Hazami M, Riahi A, Mehdaoui F, Nouicer O, Farhat A. Energetic and exergetic performances analysis of a PV/T (photovoltaic thermal) solar system tested and simulated under to Tunisian (North Africa) climatic conditions. Energy 2016;107:78–94.
[13] Ghadiri M, Sardarabadi M, Pasandideh-fard M, Moghadam AJ. Experimental investigation of a PVT system performance using nano ferrofluids. Energy Convers Manag 2015;103:468–76.
[14] Sardarabadi M, Passandideh-Fard M. Experimental and numerical study of metal-oxides/water nanofluids as coolant in photovoltaic thermal systems (PVT). Sol Energy Mater Sol Cells 2016;157:533–42.
[15] Wu X, Wu H, Cheng P. Pressure drop and heat transfer of Al2O3-H2O nanofluids through silicon microchannels. J Micromech Microeng 2009;19(10):105020.
[16] Mahendran M, Lee G, Sharma K, Shahrani A, Bakar R. Performance of evacuated tube solar collector using water-based titanium oxide nanofluid. J Mech Eng Sci 2012;3:301–10.
[17] Said Z, Sabiha MA, Saidur R, Hepbasli A, Rahim NA, Mekhilef S, et al. Performance enhancement of a flat plate solar collector using titanium dioxide nanofluid and polyethylene glycol dispersant. J Clean Prod 2015;92:343–53.
[18] Al-Shamani AN, Sopian K, Mat S, Hasan HA, Abed AM, Ruslan MH. Experimental studies of rectangular tube absorber photovoltaic thermal collector with various types of nanofluids under the tropical climate conditions. Energy Convers Manag 2016;124:528–42.
[19] Elmir M, Mehdaoui R, Mojtabi A. Numerical simulation of cooling a solar cell by forced convection in the presence of a nanofluid. Energy Proced 2012;18:594–603.
[20] Xu Z, Kleinstreuer C. Concentration photovoltaic–thermal energy co-generation system using nanofluids for cooling and heating. Energy Convers Manag 2014;87:504–12.
[21] Khanjari Y, Kasaeian AB, Pourfayaz F. Evaluating the environmental parameters affecting the performance of photovoltaic thermal system using nanofluid. Appl Therm Eng 2017;115:178–87.
[22] Leong K, Saidur R, Mahlia T, Yau Y. Entropy generation analysis of nanofluid flow in a circular tube subjected to constant wall temperature. Int Commun Heat Mass Transf 2012;39(8):1169–75.
[23] Bianco V, Manca O, Nardini S. Entropy generation analysis of turbulent convection flow of Al_2O_3–water nanofluid in a circular tube subjected to constant wall heat flux. Energy Convers Manag 2014;77:306–14.
[24] Mahian O, Kianifar A, Kleinstreuer C, Moh'd AA-N, Pop I, Sahin AZ, et al. A review of entropy generation in nanofluid flow. Int J Heat Mass Transf 2013;65:514–32.
[25] Alim MA, Abdin Z, Saidur R, Hepbasli A, Khairul MA, Rahim NA. Analyses of entropy generation and pressure drop for a conventional flat plate solar collector using different types of metal oxide nanofluids. Energy Build 2013;66:289–96.
[26] Said Z, Saidur R, Rahim NA, Alim MA. Analyses of exergy efficiency and pumping power for a conventional flat plate solar collector using SWCNTs based nanofluid. Energy Build 2014;78:1–9.
[27] Vijayalakshmi M, Rekha L, Natarajan E. Entropy generation analysis of 10Wp photovoltaic thermal hybrid system. Conference entropy generation analysis of 10Wp photovoltaic thermal hybrid system, vol. 766. Trans Tech Publ; 2015. p. 1174–9.
[28] Sardarabadi M, Passandideh-Fard M, Zeinali Heris S. Experimental investigation of the effects of silica/water nanofluid on PV/T (photovoltaic thermal units). Energy 2014;66:264–72.
[29] Drexler S, Faria J, Ruiz MP, Harwell JH, Resasco DE. Amphiphilic nanohybrid catalysts for reactions at the water/oil interface in subsurface reservoirs. Energy & Fuels 2012;26(4):2231–41.
[30] Wang C-y, Groenzin H, Shultz MJ. Comparative study of acetic acid, methanol, and water adsorbed on anatase TiO_2 probed by sum frequency generation spectroscopy. J Am Chem Soc 2005;127(27):9736–44.
[31] Li X, Li F. Study of Au/Au^{3+}-TiO_2 photocatalysts toward visible photooxidation for water and wastewater treatment. Environ Sci Technol 2001;35(11):2381–7.
[32] Huang J-Y, Liu K, Guan J-P, Tang R-C. UV protection and antibacterial properties of knitted poly (lactic acid) fabric coated with nano-ZnO. 2015.
[33] Cho S, Jang J-W, Jung S-H, Lee BR, Oh E, Lee K-H. Precursor effects of citric acid and citrates on ZnO crystal formation. Langmuir 2009;25(6):3825–31.
[34] Haddad Z, Abid C, Mohamad AA, Rahli O, Bawazer S. Natural convection of silica–water nanofluids based on experimental measured thermophysical properties: critical analysis. Heat Mass Transf 2016;52(8):1649–63.
[35] Drew DA, Passman SL. Theory of multicomponent fluids. Springer Science & Business Media; 2006.
[36] Granstrom M, Petritsch K, Arias AC, Lux A, Andersson MR, Friend RH. Laminated fabrication of polymeric photovoltaic diodes. Nature 1998;395(6699):257–60.
[37] Yousefi T, Veysi F, Shojaeizadeh E, Zinadini S. An experimental investigation on the effect of Al_2O_3–H_2O nanofluid on the efficiency of flat-plate solar collectors. Renew Energy 2012;39(1):293–8.
[38] Kumar R, Rosen MA. Performance evaluation of a double pass PV/T solar air heater with and without fins. Appl Therm Eng 2011;31(8):1402–10.
[39] Mahian O, Kianifar A, Sahin AZ, Wongwises S. Entropy generation during Al_2O_3/water nanofluid flow in a solar collector: effects of tube roughness, nanoparticle size, and different thermophysical models. Int J Heat Mass Transf 2014;78:64–75.
[40] Li Q, Xuan Y. Experimental investigation on heat transfer characteristics of magnetic fluid flow around a fine wire under the influence of an external magnetic field. Exp Therm Fluid Sci 2009;33(4):591–6.
[41] Lajvardi M, Moghimi-Rad J, Hadi I, Gavili A, Isfahani TD, Zabihi F, et al. Experimental investigation for enhanced ferrofluid heat transfer under magnetic field effect. J Magn Magn Mater 2010;322(21):3508–13.
[42] Nkurikiyimfura I, Wang Y, Pan Z. Heat transfer enhancement by magnetic nanofluids—a review. Renew Sustain Energy Rev 2013;21:548–61.
[43] Ghofrani A, Dibaei M, Sima AH, Shafii M. Experimental investigation on laminar forced convection heat transfer of ferrofluids under an alternating magnetic field. Exp Therm Fluid Sci 2013;49:193–200.
[44] Gang P, Huide F, Tao Z, Jie J. A numerical and experimental study on a heat pipe PV/T system. Sol energy 2011;85(5):911–21.
[45] Al-Salaymeh A, Al-Hamamre Z, Sharaf F, Abdelkader M. Technical and economical assessment of the utilization of photovoltaic systems in residential buildings: the case of Jordan. Energy Convers Manag 2010;51(8):1719–26.